



Unusual Pd(III) Oxidation State in Pd-Cl Chain Complex with Highly Thermal Stability and Electrical Conductivity

Journal:	<i>Dalton Transactions</i>
Manuscript ID	DT-ART-11-2020-003848.R1
Article Type:	Paper
Date Submitted by the Author:	03-Dec-2020
Complete List of Authors:	<p>Mian, Mohammad; Tohoku University, Department of Chemistry, Graduate School of Science Wakizaka, Masanori; Tohoku University, Department of Chemistry Yoshida, Takefumi; Tohoku University, WPI-Advanced Institute for Materials Research Iguchi, Hiroaki; Tohoku University Takaishi, Shinya; Tohoku University, Department of Chemistry, Graduate School of Science Afrin, Unjila; Tohoku University, Department of Chemistry Miyamoto, Tatsuya; The university of Tokyo, Applied Physics Okamoto, Hiroshi; The university of Tokyo, Applied Physics Tanaka, Hisaaki; Nagoya University, Department of Applied Physics Kuroda, Shin-ichi; Nagoya University Breedlove, Brian. K.; Tohoku University Yamashita, Masahiro; Tohoku University, Chemistry</p>

ARTICLE

Unusual Pd(III) oxidation state in Pd-Cl chain complex with highly thermal stability and electrical conductivity

Received 00th January 20xx,
Accepted 00th January 20xx

Mohammad Rasel Mian,^a Masanori Wakizaka,^{*,a} Takefumi Yoshida,^a Hiroaki Iguchi,^{*,a} Shinya Takaishi,^a Unjila Afrin,^a Tatsuya Miyamoto,^b Hiroshi Okamoto,^b Hisaaki Tanaka,^c Shin-ichi Kuroda,^c Brian K. Breedlove,^a and Masahiro Yamashita^{*,a,d}

DOI: 10.1039/x0xx00000x

The Pd(III) oxidation state is unusual and unstable since it strongly tends to disproportionate. We synthesized the quasi-one-dimensional (1D) halogen-bridged Pd(III)–Cl complex [Pd(dabdOH)₂Cl]₂ (**1-Cl**; dabdOH = (2*S*,3*S*)-2,3-diaminobutane-1,4-diol) with multiple hydrogen bonds. From single-crystal X-ray diffraction, the bridging Cl[−] ions were located at the midpoint of the Pd–Cl–Pd moieties in the 1D chains, indicating that the Pd ions are in a Pd(III) average valence (AV) state. Moreover, bright spots for the Pd(III) *d*_{z²} orbitals in the upper Hubbard band above the Fermi level were observed every ~5 Å using scanning tunnelling microscopy. These results clearly indicate that the Pd ions are in a Pd(III) AV state in **1-Cl**. In addition, **1-Cl** has the highest thermal stability (470 K) among the Pd(III) complexes reported and the highest electrical conductivity (0.6 S cm^{−1} at 300 K) among the 1D Pd-Cl chains reported so far.

Introduction

Stabilizing unusual oxidation states of metal ion has been attractive research targets because of its potential application to catalysis and functional materials. Palladium is one of the most investigated metal elements, and Pd(0), Pd(II) and Pd(IV) states have been well studied due to their crucial roles in cross coupling reactions.¹ In contrast to these oxidation states, Pd(III) state has been quite rare. As the Pd(III) state is unstable, palladium trifluoride (PdF₃) is known to exist in a mixed valence (MV) state of Pd(II) and Pd(IV).² Therefore molecular-based strategies are essential for inhibiting the disproportionation. In this context, some metal complexes with Pd ions in a +3 oxidation state have been reported.^{3–11} Cotton *et al.* have reported the di-nuclear Pd(III) compound *cis*-[Pd^{III}₂(C₆H₄PPh₂)₂(O₂CR)₂Cl₂] (R = Me, CF₃, CMe₃).⁹ These compounds are stabilized via a Pd–Pd bond since the radical spins on the *d*⁷ Pd(III) ions bind to each other. Mirica *et al.* have reported the mono-nuclear complex [Pd^{III}(N₄-L)(R)(X)]⁺ (N₄-L = *N,N'*-di-*tert*-butyl-2,11-diaza[3.3](2,6)pyridinophane; R = Me, Ph; X = Cl, Me) of which the Pd(III) state is stabilized by the steric properties of the tetradentate N₄-L ligand.¹⁰ Moreover, a semiconducting one-dimensional (1D) chain compound with

Pd(III) ions has been reported by Ritter *et al.*¹¹ In this 1D chain, the Pd(III) state is stabilized via polymeric Pd–Pd bonds both in solution and in the solid state. In these studies, the disproportionation of Pd(III) has been inhibited, whereas a higher thermal stability at room temperature or more is still elusive.

On the other hand, Pd(III) state was realized as the high pressure phase (> 20 kbar) in the Pd-Br type quasi-1D halogen-bridged metal complex (MX chain¹²) [Pd(chxn)₂Br]₂Br₂ (chxn = 1*R*,2*R*-diaminocyclohexane).¹³ At ambient pressure, Pd(II/IV) MV state in charge-density-wave state is the ground state and is characterized by two different Pd–Br bond lengths (*d*(Pd(II)–Br) and *d*(Pd(IV)–Br)) because of the double-minimum potential about the location of the bridging halogen ions. The applied pressure shrank Pd–Br–Pd distance (*d*(Pd–Br–Pd)), resulting in the single-minimum potential to afford uniformed *d*(Pd–Br). Therefore, the physical pressure induces the phase transition to Pd(III) average valence (AV) state of Mott-Hubbard state. Since Ni(III) AV state exhibits unique physical properties such as gigantic third-order nonlinearities¹⁴ and ultrafast optical switching,¹⁵ the realization of the Pd(III) state at ambient condition is important for developing solid-state functionalities of Pd(III) complexes. Thus, we introduced the chemical pressure in the crystal. The van der Waals interactions between the long alkyl chains in counteranions acted as the chemical pressure, and the Pd(III) AV state was realized at ambient pressure.^{16–18} Moreover, the multiple hydrogen bonds among ligands and counteranions shrank *d*(Pd–Br–Pd) more drastically.^{19,20} In [Pd(dabdOH)₂Br]₂Br₂ (**1-Br**; dabdOH = (2*S*,3*S*)-2,3-diaminobutane-1,4-diol), the Pd(III) state was stable up to 443 K,¹⁹ exhibiting the highest thermal stability among the Pd(III) metal complexes reported so far. In contrast, Pd(III) AV state has not been realized yet in Pd-Cl chains because it is more difficult to shrink *d*(Pd–Cl–Pd) by applying pressure in the harder Cl–

^a Department of Chemistry, Graduate School of Science, Tohoku University, 6-3 Aza-Aoba, Aramaki, Sendai 980-8578, Japan.

^b Department of Advanced Material Science, Graduate School of Frontier Sciences, The University of Tokyo, Kashiwa 277-8561, Japan.

^c Department of Applied Physics, Graduate School of Engineering, Nagoya University, Chikusa, Nagoya 464-8603, Japan.

^d School of Materials Science and Engineering, Nankai University, Tianjin 300350, China.

Electronic Supplementary Information (ESI) available: Crystallographic parameters, Schematic band structure, Optical gap data, Arrhenius plot, Seebeck coefficient plot, Spin susceptibility, Simulation for the distribution of chain length. See DOI: 10.1039/x0xx00000x

bridged system. As Cl^- ion has a higher electronegativity and a smaller ionic radius than Br^- ion does, strong hydrogen-bonding interaction and dense molecular packing are expected in Pd-Cl chains, which should have a higher thermal stability of Pd(III) state.

In this study, our aim was to realize Pd(III) state in a Pd-Cl chain and to increase its thermal stability more than that in Pd-Br chains. For this purpose, $[\text{Pd}(\text{dabOH})_2\text{Cl}]\text{Cl}_2$ (**1-Cl**) with multiple hydrogen bonding network was synthesized. Photophysical, electroconductive, and magnetic properties of **1-Cl** in the solid state were investigated.

Experimental

Materials

PdCl_2 , KCl, L(+)-tartaric acid, and $\text{CuSO}_4 \cdot 5\text{H}_2\text{O}$ were purchased from Fujifilm Wako Pure Chemical Corp. Methanol (MeOH) and acetone were purchased from Kanto Chemical Co., Inc. The ligand of dabOH was synthesized from L(+)-tartaric acid following previously reported literature.¹⁹

Synthesis

$[\text{Pd}(\text{dabOH})_2]\text{Cl}_2$. PdCl_2 (150 mg, 0.85 mmol) was dissolved in 20 mL of water. To the solution was added dabOH (215 mg, 1.77 mmol), and the solution was stirred for 3 h at 50 °C. The resulting clear solution was filtered. The solvent was removed under reduced pressure. The crude solid was dissolved into minimum amount of water, and then an excess amount of acetone was added. The resulting white precipitate was collected by using filtration. $[\text{Pd}(\text{dabOH})_2]\text{Cl}_2$ was obtained in 92% yield. Elementary analysis, Calcd for $\text{C}_8\text{H}_{24}\text{Cl}_2\text{N}_4\text{O}_4\text{Pd}$: C 23.01, H 5.79, N 13.42, found C 23.14, H 5.71, N 13.43.

$[\text{Pd}(\text{dabOH})_2\text{Cl}]\text{Cl}_2$ (1-Cl**)**. Single crystals of **1-Cl** were synthesized by using electrochemical oxidation in $\text{H}_2\text{O}/\text{MeOH}$ (6:7, 1.3 mL) solutions of $[\text{Pd}(\text{dabOH})_2]\text{Cl}_2$ (6.0 mg, 0.014 mmol) with KCl (60 mg, 0.80 mmol) at a constant current 10 μA for 2–3 days under ambient temperature and atmosphere. Yellow rod-like single crystals were obtained on the anode (Yield: 38%). Elementary analysis (%) Calcd for $\text{C}_8\text{H}_{24}\text{Cl}_3\text{N}_4\text{O}_4\text{Pd}$: C 21.21, H 5.34, N 12.37, Cl 23.48, found C 21.23, H 5.46, N 12.34, Cl 23.68.

Measurements

Electrocrystallization was carried out by using direct current multisources (YAZAWA CS-12Z) and ϕ 0.3 mm electrodes made from platinum-iridium alloy wires (Pt:Ir = 80:20). The elemental analyses were performed by using J-Science Lab Co. Ltd. JM11 at the Research and Analytical Center for Giant Molecules (Tohoku Univ.) Polarized Raman spectra were performed on a Renishaw Raman spectrometer with He-Ne laser (632.8 nm) and an optical microscope. An optical cryostat (Iwatani GAS, Mini Stat) was used for measurements below room temperature. Scanning tunneling microscopy (STM) current images were recorded on JEOL JSPM-5200 using a Pt/Ir probe under atmospheric pressure at room temperature. Ultraviolet/visible/near-infrared (UV-vis-NIR) spectra were

acquired on a Shimadzu UV-3100 instrument at RT. The temperature dependence of the electrical resistivity was measured in a liquid He cryostat of a Quantum Design PPMS (Physical Property Measuring System) MODEL 6000 by using a four-contact probe method with a typical cooling rate of 1 K/min. The electrical leads were attached to a single crystal using carbon paste (Dotite XC-12 in diethyl succinate). Measurements were carried out on several high-quality single crystals of various sizes to check the reproducibility of the resistivity data. The Seebeck measurements on **1-Cl** were performed by using a home-made device assembled from voltmeter probes, aluminum contacts, a glass substrate and a Peltier element. Electron spin resonance (ESR) spectra were measured by using a Bruker EMX spectrometer equipped with a gas-flow type cryostat Oxford ESR 900. The absolute magnitude of the spin susceptibility was calibrated using $\text{CuSO}_4 \cdot 5\text{H}_2\text{O}$ as a standard. Differential scanning calorimetry (DSC) was performed on a Shimadzu DSC-60 Plus instrument. Thermogravimetry-differential thermal analysis (TG-DTA) was performed on a Shimadzu DTG-60H instrument.

Collection of crystallographic data and structure refinements

Single-crystal X-ray diffraction data were collected on a Bruker APEX-II diffractometer with an APEX II CCD detector and JAPAN Thermal Engineering Co., Ltd Cryo system DX-CS190LD. The crystal structures were solved by using direct methods (SHELXS-97),²¹ followed by Fourier syntheses. Structure refinement was performed by using full matrix least-squares procedures using SHELXL²² on F^2 in the Yadokari-XG2009 software.²³ The X-ray crystallographic coordinates for **1-Cl** have been deposited at the Cambridge Crystallographic Data Centre (CCDC) under deposition numbers CCDC-2038345 (100 K) and CCDC-2038346 (350 K).

Results and discussion

Synthesis and crystal structure of **1-Cl**

The precursor Pd(II) complex $[\text{Pd}(\text{dabOH})_2]\text{Cl}_2$ was synthesized through a complexation reaction between PdCl_2 and the dabOH ligands. Complex **1-Cl** was obtained as brown needle-like crystals by using electrochemical oxidation from $[\text{Pd}(\text{dabOH})_2]\text{Cl}_2$ (Figure 1). Figure 2 shows a crystal structure of **1-Cl** at 100 K obtained using single-crystal X-ray diffraction, and the crystallographic data are summarized in Table S1. From structural analysis, **1-Cl** has an MX-chain structure of $-\text{Pd}-\text{Cl}-$ along the b -axis. The Pd-Cl chain structure indicates that the 1D electron system is composed of the Pd $4d_{z^2}$ orbitals and the Cl $3p_z$ orbitals. Two dabOH ligands are chelated to the Pd center at the equatorial positions. Moreover, the Cl^- was accurately located at the midpoint of the Pd-Cl-Pd moieties ($d(\text{Pd}-\text{Cl}) = 2.473(5)$ and $2.474(5)$ Å) in the chains, suggesting that the Pd ions are in a +3 AV state. Besides the bridging Cl^- ions in the chains, Cl^- counteranions (Cl_v) bridge four $[\text{Pd}(\text{dabOH})_2]^{3+}$ units by intra- and interchain hydrogen bonding. The shortest hydrogen bond is $3.078(4)$ Å for $\text{O}\cdots\text{Cl}_v$ and $3.287(8)$ Å for $\text{N}\cdots\text{Cl}_v$. As the result of the multiple hydrogen bonds, the distance $d(\text{Pd}-$

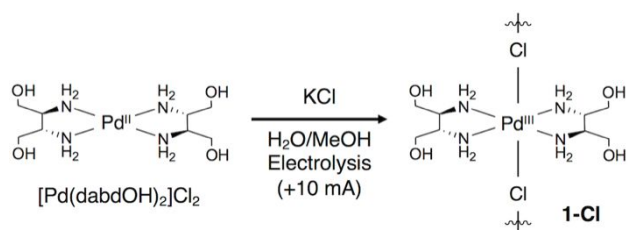


Figure 1. Synthetic scheme for 1-Cl.

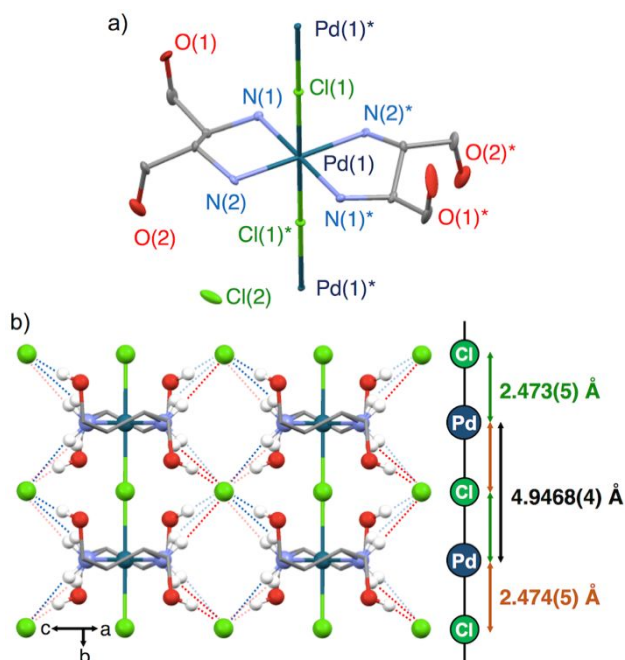


Figure 2. Crystal structure of 1-Cl: (a) ORTEP diagram at the 50% probability level without the H-atoms for clarity, and (b) a ball-and-stick model with hydrogen-bond networks indicated and selected distances. Blue and red dotted lines show hydrogen bonds. Color code: Pd = navy, Cl = green, O = red, N = light blue, and C = gray.

$\text{Cl}-\text{Pd}$ was $4.9468(4) \text{ \AA}$, which is the shortest value to date. For comparison, $d(\text{Pd}-\text{Cl}-\text{Pd})$ has been reported to be 5.164 \AA for $[\text{Pd}(\text{chxn})_2\text{Cl}]\text{Cl}_2$ in an MV state.²⁴ Figure 3a shows the temperature dependence of $d(\text{Pd}-\text{X}-\text{Pd})$ ($\text{X} = \text{Cl}$ or Br) in 1-Cl and 1-Br,¹⁹ respectively. The $d(\text{Pd}-\text{Cl}-\text{Pd})$ increased 0.45% for 1-Cl in the temperature range of 100–350 K, whereas $d(\text{Pd}-\text{Br}-\text{Pd})$ increased 0.64% for 1-Br in a similar temperature range. The thermal robustness suggests that the multiple hydrogen bonds in 1-Cl are stronger than those in 1-Br are. The bridging Cl^- ions remained located at the midpoint between two Pd ions ($d(\text{Pd}-\text{Cl}) = 2.481(7)$ and $2.488(7) \text{ \AA}$) even at 350 K, suggesting that 1-Cl remains in a Pd(III) AV state at higher temperatures. In addition, the Cl_y counteranions crosslink the chains via interchain hydrogen bonds, forming a 2D sheet structure in the bc -plane. Since the 2D sheets stack through weak van der Waals interactions, these crystals were cleavable along the bc -planes.

Characterization for the Pd(III) average valence state

Polarized Raman spectroscopy is a powerful probe for clarifying the chemical environment. For MX chains, the symmetrical stretching mode ($\cdots\text{M}^{\text{III}}\cdots\text{X}-\text{M}^{\text{IV}}-\text{X}\cdots$) in the MV state is allowed,

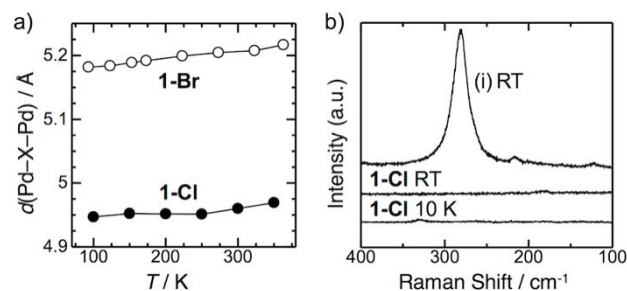


Figure 3. (a) Temperature dependence of Pd-X-Pd distance in 1-Cl (filled circle) and 1-Br (hollow circle).¹⁹ (b) Polarized Raman spectra of 1-Cl at 10 K and room temperature together with that of (i) $[\text{Pt}(\text{dabdhOH})_2\text{Cl}]\text{Cl}_2$ at room temperature.²⁶

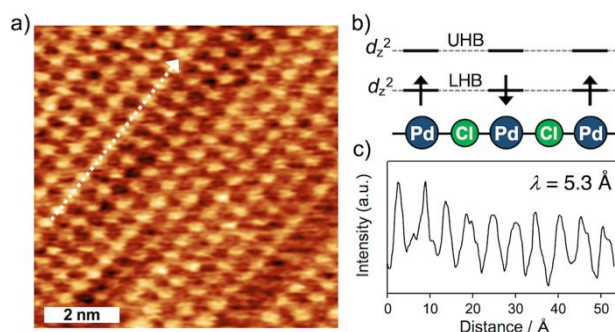


Figure 4. (a) STM image of 1-Cl in the bc -plane ($80 \times 80 \text{ \AA}^2$). The arrow indicates the 1D chain direction (b -axis). (b) Schematic energy diagram for 1-Cl. (c) The current profile for STM of 1-Cl on the dashed-arrow in (a).

whereas that in the AV state ($-\text{M}^{\text{III}}-\text{X}-$) is forbidden,^{8,16–20,24–26} because the change in the polarizability at the equilibrium position is zero when X locates at the midpoint in the AV state. Figure 3b shows polarized Raman spectra for a single crystal of 1-Cl together with that for $[\text{Pt}(\text{dabdhOH})_2\text{Cl}]\text{Cl}_2$ in an MV state. From 10 K up to room temperature, no signal was observed in the range of 100–400 cm^{-1} in the spectra of 1-Cl, whereas in the case of $[\text{Pt}(\text{dabdhOH})_2\text{Cl}]\text{Cl}_2$ in the MV state, a signal has been observed.²⁶ The absence of the symmetric mode strongly indicates that 1-Cl is in an AV state. In addition, Figure 4 shows a STM image for 1-Cl at room temperature at atmospheric pressure with a positive sample bias (150 mV). In the image, a periodic structure of oriented dots with mean interval distances between the bright spots of ~ 5 and $\sim 7 \text{ \AA}$, which are consistent with the $\text{Pd}\cdots\text{Pd}$ distance along the b -axis (4.95 \AA) and c -axis (7.17 \AA) obtained from X-ray structure, respectively. The spots along the chain direction (b -axis) clearly indicate that the

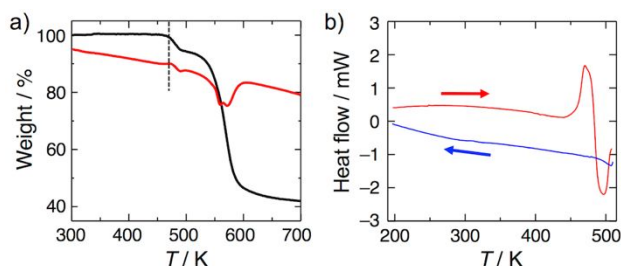


Figure 5. (a) TG (black line) and DTA (red line) traces and (b) DSC thermograms for 1-Cl at a scan rate of 10 K min^{-1} .

electrons reside in the Pd(III) d_z^2 orbitals in the upper Hubbard band (UHB).^{8,16,19} Thus, these results mean that the Pd ions in **1-Cl** are in an AV state at room temperature or below. Moreover, from TG-DTA and DSC, no phase transition occurred until the decomposition temperature of 470 K (Figure 5). Therefore, **1-Cl** has the highest thermal stability among the reported Pd(III) complexes so far.^{3,4,8,16–19}

Electrical and physical characteristics for **1-Cl**

In order to estimate the optical gap energy (E_{CT}) for **1-Cl**, UV-vis-NIR spectroscopy was performed using a KCl pellet, as shown in Figure 6a. A broad absorption band was observed around 1.0 eV. This broad peak was assigned to be a transition from the lower Hubbard band (LHB) to the UHB in the AV state (Figure S1). To the best of our knowledge, **1-Cl** has the smallest E_{CT} value among the reported Pd–Cl chains (Table S2).^{27–30} However, the E_{CT} value of **1-Cl** is larger than that of **1-Br** (0.45 eV),¹⁹ indicating that the optical gap is sensitive to the bridging halide ions or, in other words, the size of halide ions. As the orbital overlap between $4d_z^2$ and $3p_z$ is smaller than that of $4p_z$, **1-Cl** should have a narrower band with a wider band gap.

The temperature dependence of the electrical conductivity (σ) of a single crystal of **1-Cl** was measured under ambient pressure along the chain direction (b -axis), as shown in Figure 6b. σ increased with an increase in the temperature, meaning that **1-Cl** is a semiconductor. σ was measured to be 0.6 S cm^{-1} at 300 K, which is the highest value of σ_{rt} for Pd–Cl type MX chains ($4.3 \times 10^{-9} \text{ S cm}^{-1}$ for $[\text{Pd}(\text{NH}_3)_2\text{Cl}]\text{Cl}_2$ ²⁷ and $2.0 \times 10^{-12} \text{ S cm}^{-1}$ for $[\text{Pd}(\text{en})_2\text{Cl}](\text{ClO}_4)_2$).³¹ Moreover, σ_{rt} of **1-Cl** is even higher than those of the Ni-containing MX chains (0.1 S cm^{-1} reported for a Ni–Br chain³²). In addition, the activation energy (E_a) for **1-Cl** is determined to be 86 meV by fitting the data using the Arrhenius equation in the range of 100–300 K (Figure S2). The E_a value is much less than half of E_{CT} (475 meV), suggesting the existence of impurity levels between the LHB and UHB. As a negative Seebeck coefficient (-0.458 mV K^{-1}) was observed (Figure S3), **1-Cl** is an n-type semiconductor involving levels from Pd(II) impurities.

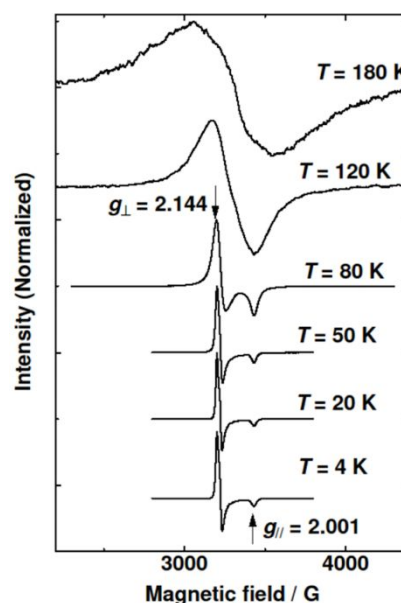


Figure 7. ESR spectra of **1-Cl** measured at various temperatures. ESR signal could not be measured over 200 K due to the extreme broadening.

ESR spectroscopy was performed using polycrystalline samples of **1-Cl** (Figures 7 and S4). The g values are $g_{\perp} = 2.144$ and $g_{\parallel} = 2.001$ at 80 K. These anisotropic values indicate that the spin is present in the Pd(III) d_z^2 orbital and are derived from domains containing odd numbers of Pd(III) ions in the chain.³ A plot of the molar spin susceptibilities (χ) obtained from the ESR spectra showed that the spin exhibited Curie-like behavior below 50 K, and the amount of the Curie spin is calculated to be

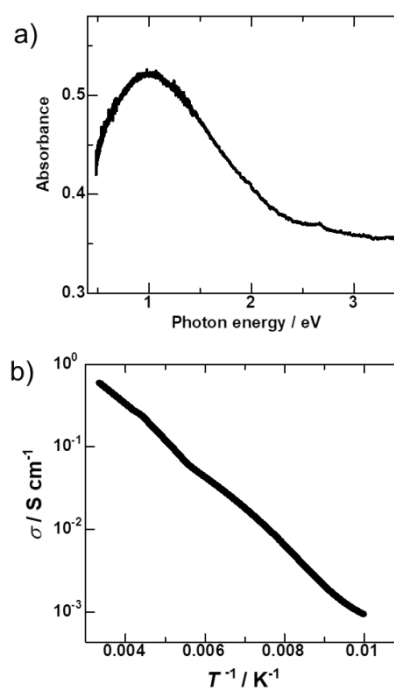


Figure 6. (a) UV-Vis-NIR absorption spectra for KCl pellets of **1-Cl** at room temperature. (b) Variable-temperature electrical conductivity (σ) of a single-crystal of **1-Cl** along the chain axis measured by using a four-contact probe method.

0.11%. Therefore, the mean length of the chains in the crystals was estimated to be 224 nm assuming a Gaussian distribution (Figure S5). It is noted that χ exhibits a clear increase from the Curie law above 50 K associating with a gradual broadening of the ESR signal. This behavior indicates a finite contribution of 1D Pd(III) spin chain, which has well demonstrated by previous investigations,^{19,20,33,34} giving a magnetic evidence of the AV state in **1-Cl**.

Conclusions

A new quasi-one-dimensional (1D) halogen-bridged Pd(III) complex, [Pd(dabdoH)₂Cl]Cl₂ (**1-Cl**), was prepared. **1-Cl** is the first example of a Pd–Cl chain with the Pd ions in a +3 average valence state. The Pd(III) state is stabilized due to the chemical pressure through multiple hydrogen bonds. In addition, this complex has the highest thermal stability (470 K) among the Pd(III) complexes reported so far as well as the highest electrical conductivity (0.6 S cm⁻¹ at 300 K) among the known 1D Pd-Cl chains.

Conflicts of interest

There are no conflicts to declare.

Acknowledgements

This work was supported by JSPS KAKENHI Grant Numbers JP15K17828 (H.I.), JP18K14233 (H.I.), JP18H04498 (H.I.), JP18J13022 (M.R.M.), JP18H01166 (H.O.) and JP19H05631 (H.I., S.T. and M.Y.), by JST CREST Grant Number JPMJCR1661 (H.O.), by the Toyota Riken Scholar Program (H.I.) and by Kato Foundation for Promotion of Science KJ-2916 (H.I.), Japan. M.Y. thanks the 111 Project (B18030) from China for the support.

Notes and references

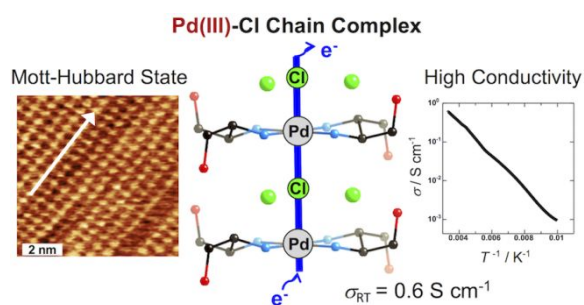
- (a) I. J. S. Fairlamb and A. F. Lee, in C-H and C-X Bond Functionalization: Transition Metal Mediation, (Ed.: X. Ribas), the Royal Society of Chemistry, Cambridge, 2013, pp. 72–107; (b) A. N. Vedernikov, in C-H and C-X Bond Functionalization: Transition Metal Mediation, (Ed.: X. Ribas), the Royal Society of Chemistry, Cambridge, 2013, pp. 108–121.
- B. G. Muller, *Angew. Chem. Int. Ed.* 1987, **26**, 1081.
- L. M. Mirica and J. R. Khusnutdinova, *Coord. Chem. Rev.* 2013, **257**, 299.
- D. C. Powers and T. Ritter, *Acc. Chem. Res.* 2012, **45**, 840.
- A. J. Blake, A. J. Holder, T. I. Hyde, Y. V. Roberts, A. J. Lavery and M. Schröder, *J. Organomet. Chem.* 1987, **323**, 261.
- A.-J. Martínez-Martínez, M.-T. Chicote, D. Bautista and J. Vicente, *Organometallics* 2012, **31**, 3711.
- F. Estevan, P. Hirva, A. Ofori, M. Sanaú, T. Špec and M. A. Úbeda, *Inorg. Chem.* 2016, **55**, 2101.
- T. Yoshida, S. Takaishi, H. Iguchi, H. Okamoto, H. Tanaka, S. Kuroda, Y. Hosomi, S. Yoshida, H. Shigekawa, T. Kojima, H. Ohtsu, M. Kawano, B. K. Breedlove, L. Guerin and M. Yamashita, *ChemistrySelect* 2016, **2**, 259.
- F. A. Cotton, I. O. Koshevoy, P. Lahuerta, C. A. Murillo, M. Sanaú, M. A. Ubeda and Q. Zhao, *J. Am. Chem. Soc.* 2006, **128**, 13674.
- J. R. Khusnutdinova, N. P. Rath and L. M. Mirica, *J. Am. Chem. Soc.* 2010, **132**, 7303.
- M. G. Campbell, D. C. Powers, J. Raynaud, M. J. Graham, P. Xie, E. Lee and T. Ritter, *Nat. Chem.* 2011, **3**, 949.
- Recent representative articles of MX chains: (a) M. Yamashita, *Bull. Chem. Soc. Jpn.* DOI: 10.1246/bcsj.20200257; (b) K.-i. Otake, K. Otsubo, H. Kitagawa, *J. Phys.: Condens. Matter.* DOI: 10.1088/1361-648X/abbbc7; (c) K.-i. Otake, K. Otsubo, T. Komatsu, S. Dekura, J. M. Taylor, R. Ikeda, K. Sugimoto, A. Fujiwara, C.-P. Chou, A. W. Sakti, Y. Nishimura, H. Nakai and H. Kitagawa, *Nat. Commun.* 2020, **11**, 843; (d) U. Afrin, H. Iguchi, M. R. Mian, S. Takaishi, H. Yamakawa, T. Terashige, T. Miyamoto, H. Okamoto and M. Yamashita, *Dalton Trans.* 2019, **48**, 7828.
- K. Okaniwa, H. Okamoto, T. Mitani, K. Toriumi, M. Yamashita, *J. Phys. Soc. Jpn.* 1991, **60**, 997.
- (a) H. Kishida, H. Matsuzaki, H. Okamoto, T. Manabe, M. Yamashita, Y. Taguchi, Y. Tokura, *Nature* 2000, **405**, 929; (b) S. Tao, T. Miyagoe, A. Maeda, H. Matsuzaki, H. Ohtsu, M. Hasegawa, S. Takaishi, M. Yamashita and H. Okamoto, *Adv. Mater.* 2007, **19**, 2707.
- S. Iwai, A. Maeda, H. Matsuzaki, H. Kishida, H. Okamoto and Y. Tokura, *Phys. Rev. Lett.* 2003, **91**, 057401.
- S. Takaishi, M. Takamura, T. Kajiwara, H. Miyasaka, M. Yamashita, M. Iwata, H. Matsuzaki, H. Okamoto, H. Tanaka, S. Kuroda, H. Nishikawa, H. Oshio, K. Kato and M. Takata, *J. Am. Chem. Soc.* 2008, **130**, 12080.
- S. Kumagai, S. Takaishi, B. K. Breedlove, H. Okamoto, H. Tanaka, S. Kuroda and M. Yamashita, *Chem. Commun.* 2014, **50**, 8382.
- S. Kumagai, S. Takaishi, H. Iguchi, B. K. Breedlove, T. Kaneko, H. Ito, S. Kuroda and M. Yamashita, *Inorg. Chem.* 2018, **57**, 12.
- M. R. Mian, H. Iguchi, S. Takaishi, H. Murasugi, T. Miyamoto, H. Okamoto, H. Tanaka, S. Kuroda, B. K. Breedlove and M. Yamashita, *J. Am. Chem. Soc.* 2017, **139**, 6562.
- M. R. Mian, U. Afrin, H. Iguchi, S. Takaishi, T. Yoshida, T. Miyamoto, H. Okamoto, H. Tanaka, S. Kuroda and M. Yamashita, *CrystEngComm*, 2020, **22**, 3999.
- G. M. Sheldrick, *Acta Crystallogr.* 2008, **A64**, 112.
- G. M. Sheldrick, *Acta Crystallogr.* 2015, **C71**, 3.
- Yadokari-XG, Software for Crystal Structure Analyses, K. Wakita (2001); Release of Software (Yadokari-XG 2009) for Crystal Structure Analyses, C. Kabuto, S. Akine, T. Nemoto, E. Kwon, *J. Cryst. Soc. Jpn.* 2009, **51**, 218.
- (a) R. J. H. Clark, M. Kurmoo, D. N. Mountney and H. Toftlund, *J. Chem. Soc. Dalton Trans.* 1982, 1851; (b) H. Okamoto, T. Mitani, K. Toriumi and M. Yamashita, *Mater. Sci. Eng. B* 1992, **13**, L9; (c) H. Okamoto, K. Toriumi, T. Mitani and M. Yamashita, *Phys. Rev. B* 1990, **42**, 10381; (d) O. Hiroshi and Y. Masahiro, *Bull. Chem. Soc. Jpn.* 1998, **71**, 2023.
- T. Manabe, T. Kawashima, T. Ishii, H. Matsuzaka, M. Yamashita, K. Marumoto, H. Tanaka, S. Kuroda, H. Kitagawa, T. Mitani and H. Okamoto, *Synth. Met.* 2001, **116**, 415.
- M. R. Mian, H. Iguchi, S. Takaishi, U. Afrin, T. Miyamoto, H. Okamoto and M. Yamashita, *Inorg. Chem.* 2019, **58**, 114.
- L. V. Interrante and K. W. Browall, *Inorg. Chem.* 1974, **13**, 1162.
- Y. Wada, T. Mitani, M. Yamashita and T. Kida, *J. Phys. Soc. Jpn.* 1985, **54**, 3143.
- N. Matsumoto, M. Yamashita and S. Kida, *Bull. Chem. Soc. Jpn.* 1978, **51**, 2334.
- H. Matsuzaki, K. Iwano, T. Aizawa, M. Ono, H. Kishida, M. Yamashita and H. Okamoto, *Phys. Rev. B* 2004, **70**, 035204.
- Y. Hamaue, R. Aoki, M. Yamashita and S. Kida, *Inorg. Chim. Acta* 1981, **54**, L13.

ARTICLE

Journal Name

- 32 S. Takaishi, M. Yamashita, H. Matsuzaki, H. Okamoto, H. Tanaka, S. Kuroda, A. Goto, T. Shimizu, T. Takenobu and Y. Iwasa, *Chem. Eur. J.* 2008, **14**, 472.
- 33 K. Marumoto, H. Tanaka, S. Kuroda, T. Manabe and M. Yamashita, *Phys. Rev. B* 1999, **60**, 7699.
- 34 H. Tanaka, K. Marumoto, S. Kuroda, T. Manabe, M. Yamashita, *J. Phys. Soc. Jpn.* 2002, **71**, 1370.

For Table of Contents Only



A thermal stable and high electrical conductive Pd(III) 1D complex $[\text{Pd}(\text{dabdOH})_2\text{Cl}]\text{Cl}_2$ was newly synthesized.